Proceedings of the
Annual Stability Conference
Structural Stability Research Council
St. Louis, Missouri, April 16-20, 2013

Compression Members with Hollow Sections and Concentric Slotted Gusset Plates – Behavior and Recommended Design Model

H. Unterweger[1], A. Taras[2]

Abstract

In practical applications, compression members in trusses or bracing systems are often composed of hollow sections with slotted gusset plates on both ends. Either a bolted connection with splice plates on both sides or a welded connection are used to achieve a concentric configuration. In recent application cases, members of this type were designed with unusually long gusset plates at their ends, leading to reduced load bearing capacities.

In the present paper, the load carrying behavior of such members is shown by means of realistic numerical calculations. The resulting compression member capacities are compared with the design models for flexural buckling as they are commonly employed in practice.

It will be shown that these models significantly overestimate the compression member capacity – particularly in cases with low slenderness. Interestingly, imperfection forms similar to the second eigenmode often lead to the most critical design situation. The influence of residual stresses due to the welding of the gusset plate to the slotted hollow section is also studied in detail.

On the basis of these numerical results, an improved engineering design recommendation for the practical verification of the gusset plate stability could be developed, which should be used in addition to the conventional member buckling verification.

1. Introduction and motivation for a comprehensive study

Members in trusses as well as members of bracings are often designed with hollow sections (rectangular – RHS or circular – CHS) and slotted gusset plates on both ends. Either a bolted connection with splice plates on both sides or a welded connection are used to achieve a concentric configuration. Two typical examples are shown in Fig. 1.

[1] Full Professor, Graz University of Technology, <h.unterweger@tugraz.at>
[2] Assistant Professor, Graz University of Technology, <taras@tugraz.at>

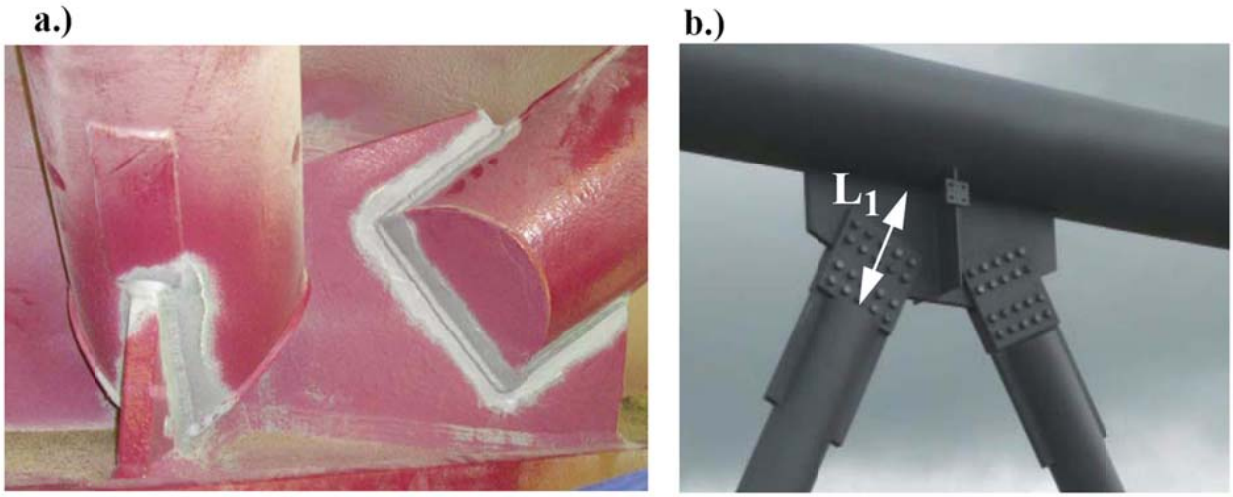

Figure 1: Examples for member joints – welded and bolted, respectively (from [1])

A bolted connection leads to a greater length L_1, with reduced bending stiffness out of plane, as is also visible in Fig. 1. Based on a study of common detailing solutions, usual values for L_1, depending on the member depth h, are given in Fig. 2.

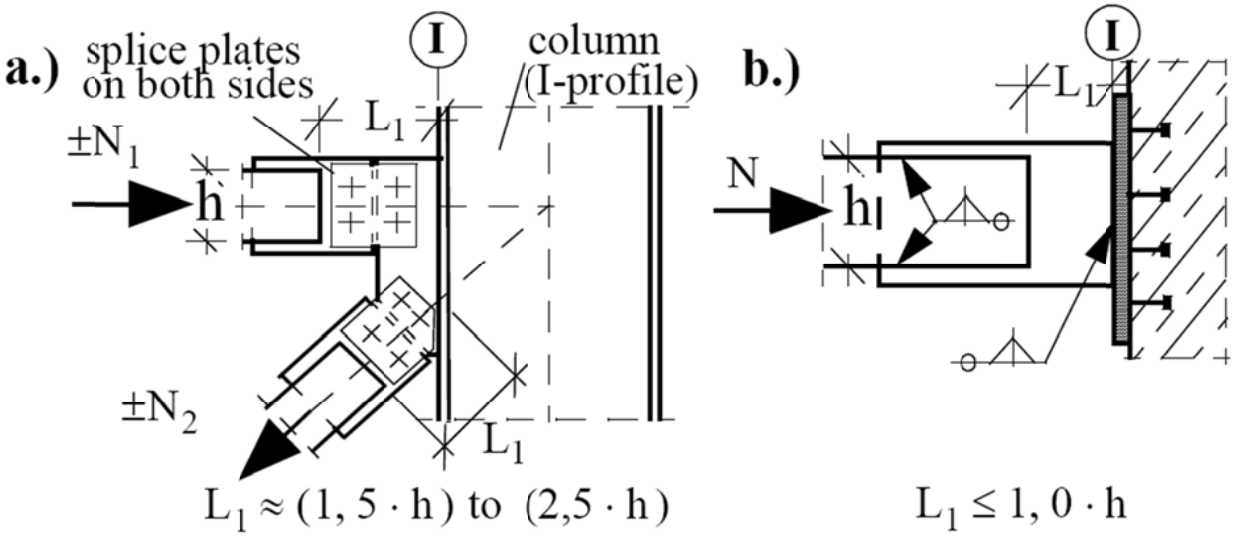

Figure 2: Studied RHS – member joints; a.) bolted, b.) welded

Fig. 2 also shows the two limiting cases for member support out of plane. In Fig. 2a in axis I, a pinned end must be assumed, whereas in Fig. 2b – a connection to a concrete wall –a practically clamped support is present. Only these two cases are studied in detail.

The authors' motivation for a comprehensive study of the behavior of compression members with slotted gusset plates was given by the fact that the literature – to the authors' knowledge – lacks a comprehensive analytical and numerical study dealing with buckling of such members. It must be pointed out that for these hollow sections out of plane flexural buckling is always predominant, which can also be interpreted as an interaction of global buckling and local buckling of the gusset plate.

Within the literature, a lot of studies are available dealing with the load transfer from the gusset plate to the hollow section (e.g. Zhao R. (2009) and references there), however the focus is placed on tension applications, excluding buckling phenomena.
In past detailing practice, the buckling resistance was sufficiently warranted by performing a buckling check for the hollow section itself, since the gusset plates were usually very short and had a negligible effect on the buckling length and/or were not the subject to significant second-order out of plane bending. However, more recent detailing practice led to free lengths L_1 of the gusset plates that are significantly larger than old design tradition.
As will be shown in the following, the limited cross-sectional bending capacity of the gusset plate can also lead to a significant reduction of the overall compression strength of the member. Only for very slender members a conventional buckling verification – even when taking account of the potentially increased buckling length due to the reduced bending stiffness in the joint region – is sufficient to guarantee structural safety.

If, in addition to a long gusset plate, an eccentric joint configuration is chosen (e.g. directly bolted without splice plates) a further, significant reduction of the member compression capacity is observed. In this case design recommendations are given in Unterweger (2010).

2. Simplifications and parameter range of the study

In order to study the load bearing capacity of hollow sections with slotted gusset plates on both ends, some simplifications were introduced, shown in Fig. 3. In this figure, the studied geometry with the chosen symbols and notations is presented as well. The two studied border cases for boundary conditions of the gusset plate are: - pinned (BC1) and, - fully clamped (BC2) ends, with rigid support out of plane (in both cases).

In the study described here, squared hollow sections were analyzed, ignoring the fillets at the edges ($b = h$) and leading to the area A_0, second moment of area J_{z0} and radius of gyration r_{z0}. However, the final results can be shown to also be valid for rectangular and circular hollow sections. The free length L_1 of the gusset plate was varied between $L_1 = 1{,}0 \cdot h \div 2{,}0 \cdot h$. The height of the gusset plate h_1 was fixed with $h_1 = 1{,}3 \cdot h$, which is typical for practical applications.

The slotted length L_s, which was chosen to be $L_s = 1{,}75 \cdot h$, is of great significance and represents a minimum value: this length is at least necessary in order to utilize the full axial and bending capacity of the member at the end of the gusset plate, due to the load introduction from the gusset plate into the hollow section. This was also verified within the comprehensive FEM-study, which will be presented in section 4.

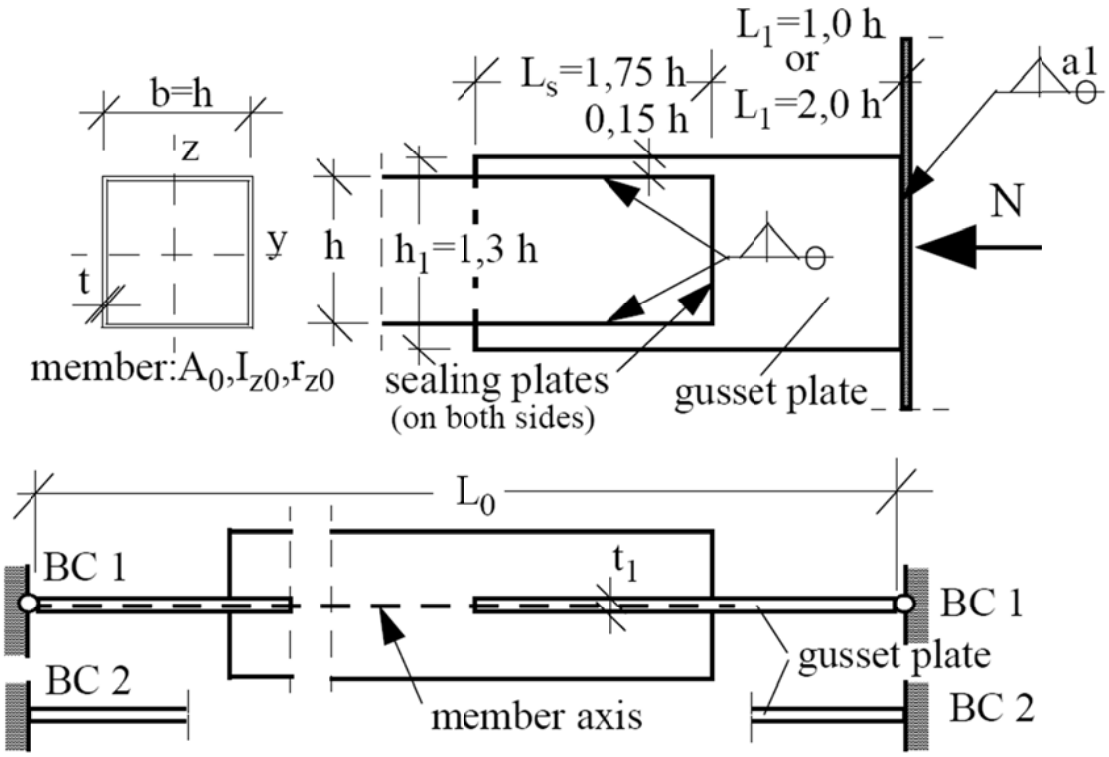

Figure 3: Sketch of studied joint configuration; geometry and idealized boundary conditions

2.1 Relevant stiffness ratio I_1/I_0 and member length ratio L_1/L_0

The buckling capacity of the member strongly depends on the stiffness ratio I_1/I_0 of the gusset plate (I_1 according to Eq. 1) and member ($I_0 = I_{z0}$)

$$I_1 = \frac{h_1 \cdot t_1^3}{12} \tag{1}$$

Based on the assumed geometry of the gusset plates ($h_1 = 1{,}3 \cdot h$) and quadratic RHS-sections used in Europe for the stiffness ratio I_1/I_0, Eq. (2) is valid (h = depth and t = thickness of the member respectively; A_0 = area of the member, A_1 = area of the gusset plate)

$$\frac{I_1}{I_0} = 4{,}68 \cdot \left(\frac{t}{h}\right)^2 \cdot \left(\frac{A_1}{A_0}\right)^3 \tag{2}$$

In practice, $A_1 \sim A_0$ is often valid leading to very small stiffness ratios of about $I_1/I_0 \sim 0{,}01$.

Another important parameter is the member length ratio L_1/L_0. For practical cases, $L_1/L_0 = 0{,}05 \div 0{,}10$ is often valid.

2.2 Loading of the member

In this study, only constant axial compression forces are considered. Geometric imperfections were taken into account, based on execution tolerances. The effect of residual stresses was also

studied, in particular those residual stresses caused by the welded connection between member and gusset plate.

3. Buckling verification in practice and danger of overestimation of member capacity

3.1 Buckling verification in practice

Due to the significantly reduced bending stiffness of the gusset plate at the end of the member (length L_1), for the buckling verification of the member out of plane – based on a constant bending stiffness $I_{z,0}$ over the whole length L_0 – an increased effective length $L_{cr} = \beta \cdot L_0$ must be used. This is illustrated in Fig. 4. For members with slotted gusset plates, sometimes the second buckling mode is relevant for the ultimate buckling strength of the member, so that $L_{cr,2}$ based on β_2 replaces $L_{cr,1}$ calculated with β_1.

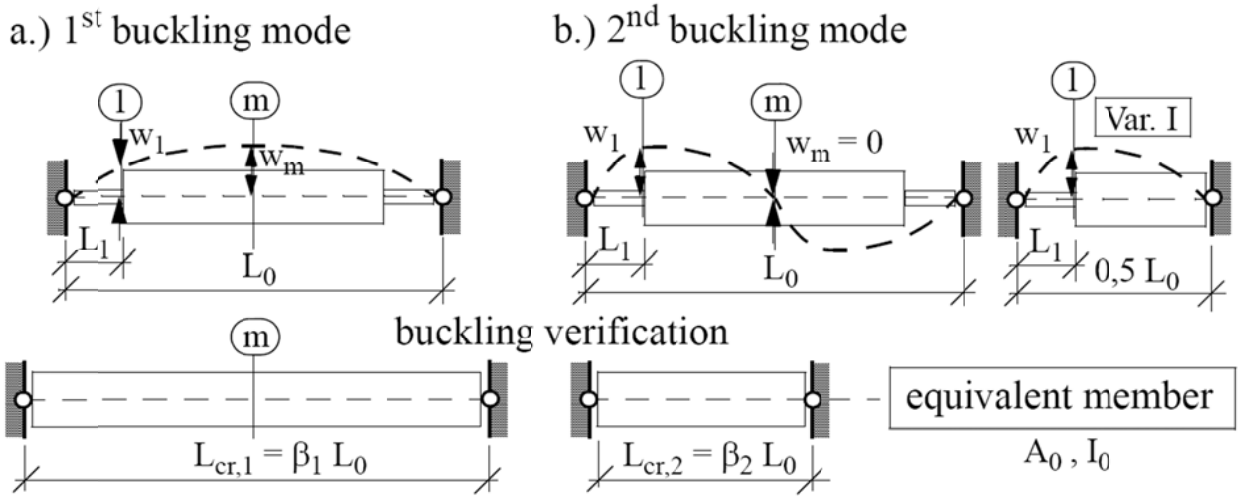

Figure 4: a.) First and b.) second bifurcation buckling mode shapes and the associated equivalent columns

The relationship between effective length and ideal buckling load N_{cr} for each mode i is given by the well known Eq. (3)

$$N_{cr,i} = \frac{\pi^2 \cdot E \cdot J_{z0}}{(\beta_i \cdot L_0)^2} \tag{3}$$

In the literature, a number of analytic formulas for an iterative solution for the effective length factors β_i and ideal buckling loads $N_{cr,i}$ can be found (Pflüger (1964)). Simplified solutions (Dimitrov (1953), also found in Petersen (1982)), lead to very unsafe results. Appropriate analytical formulas for the studied cases (see Fig. 4) are summed up by the authors in Unterweger, Taras (2011).

For practical applications, all the relevant results for the effective length factors β_i are summed up in Fig. 5. In these figures, the parameter I is equal to the stiffness ratio ($I = I_1/I_0$). The results are plotted for I = 0,01 , 0,02 and 0,04, covering all practical cases.

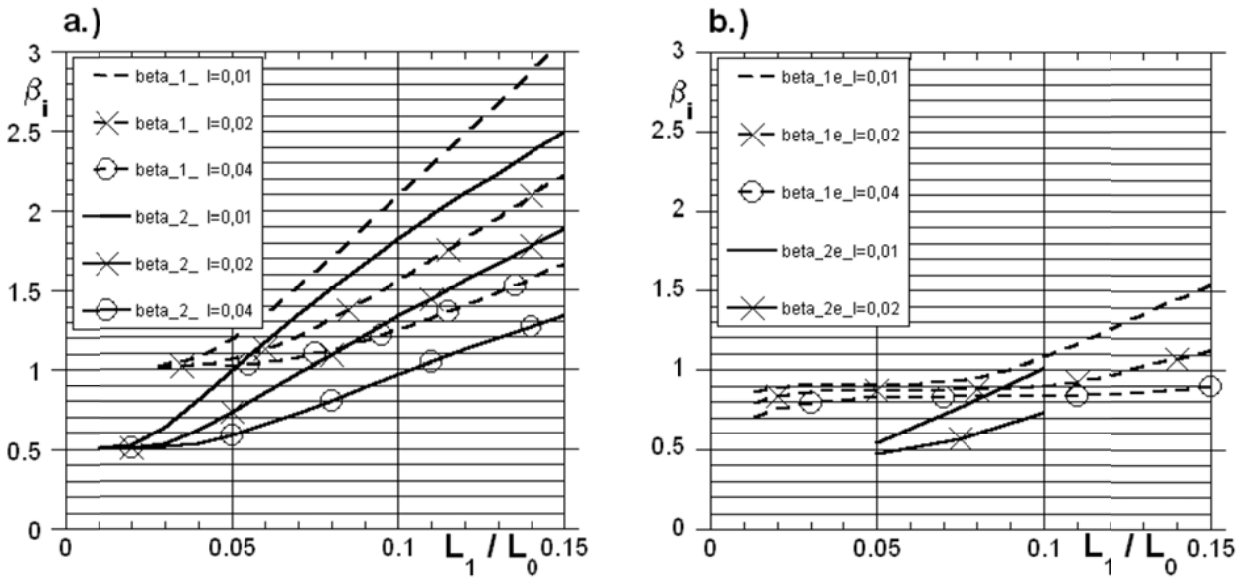

Figure 5: Factors β_i for the determination of buckling lengths (1st and 2nd buckling mode) using the equivalent member for, a.) pinned ends and b.) fixed ends

3.2 Overestimation of the buckling strength of a member with slotted gusset plate

Before all the details and results of the comprehensive study are presented in the following section, a simplified example is shown, in order to emphasize the significant difference in buckling behavior when compared to a simply supported constant-section member (section $I_{z,0}$ over whole length L_0).

Fig. 6 shows an alternative approach for the calculation of the ultimate compression strength of a simply supported member. Based on an equivalent imperfection e_{equ} and application of second order theory, the internal forces at the relevant section m ($N = P$, $M = P \cdot w$) are calculated. The increased deformation w depends on the actual load P and the ideal buckling load P_{cr}, using the well-known second-order elastic amplification factor f_{II} in Eq. (4).

$$f_{II} = \frac{1}{1 - P/P_{cr}} \tag{4}$$

Making use of the (elastic) member capacity in section m ($\sigma_{max} = F_y$), the ultimate compression strength of the member can be determined analytically from second-order theory. Some codes, like the Eurocode (2012), give formulas for e_{equ} that lead to the same compression strength of the member as the one given by the buckling curves codified in the same standard.

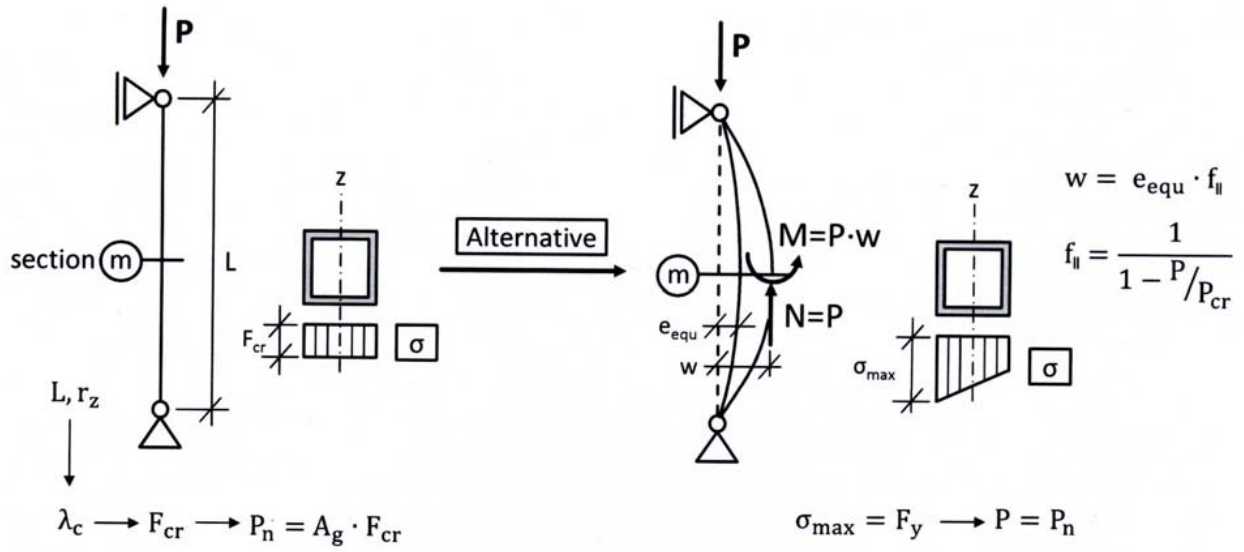

Figure 6: Compressive Strength of a column – alternative approach

Based on the second order theory approach in Fig. 6, it is now possible to show the utilization of the relevant gusset-plate section capacity in axis 1. In Fig. 7, a typical example of a hollow section member (RHS: h = b = 200, t = 10 mm) of length L_0 = 8000 mm is shown.

The member compression strength of P_n = 840 kN given in Fig. 7a is based on the proposed verification in Fig. 4, using the effective length factors β_1 in Fig. 5 and the buckling curve a of the Eurocode (2012). The shape of the imperfections is based on the 1st buckling eigenmode (simplified in a sine-wave form) in Fig. 7a and on the 2nd mode (simplified, with e_{equ} in section 1 of Fig. 7) in Fig. 7b.

When the load is thus set equal to the theoretical resistance P_n = 840 kN, only the hollow member has sufficient section capacity. In the gusset plate section 1 – particularly for the imperfections based on the 2nd mode – the utilization factors UF_1 are significantly higher than 1, and this even if the increased plastic section capacity is used ($UF_{1,pl}$).

This means that the compression strength based on the buckling verification of the member with increased, equivalent buckling length (see Fig. 4) significantly overestimates the buckling capacity of the member with slotted gusset plates, because the gusset plate section 1 (and not the mid-span cross-section of the HS member) determines the ultimate capacity, as well as the fact that imperfections based on the 2nd mode must also be considered.

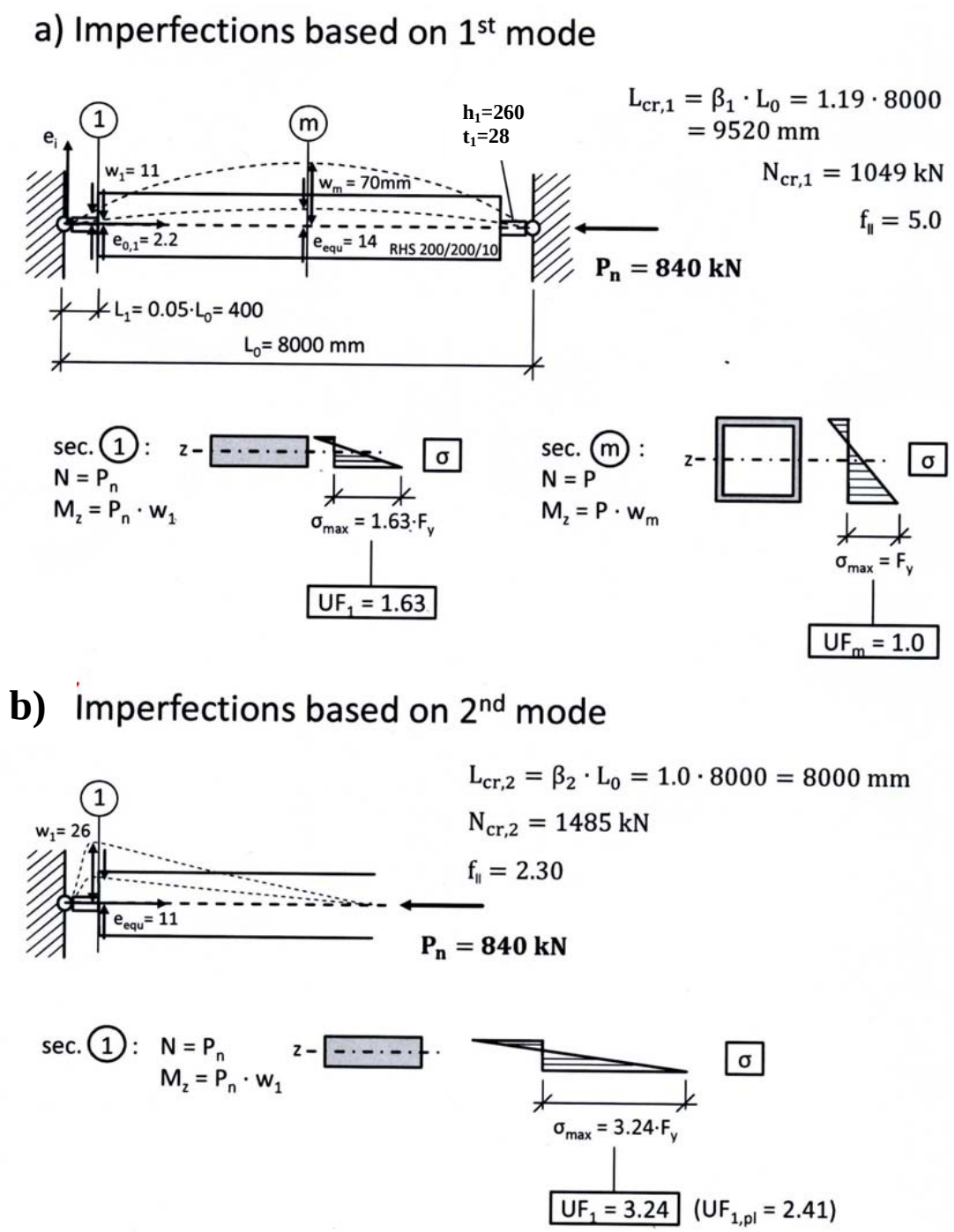

Figure 7: Practical example of a hollow section member with slotted gusset plates; Reduced buckling strength due to reduced section capacity in section 1 of the gusset plate

4. Simulation of the realistic load bearing behavior of members with slotted gusset plates

The realistic load bearing behavior of members with slotted gusset plates, shown in Fig. 3, was studied in detail, based on numerical FEM-calculations.

4.1 FEM-model

The numerical calculations were done with the Finite Element Software ABAQUS. In Fig. 8 the FEM-model at the member end is shown. A combination of volume, shell and beam elements was chosen. The gusset plates were modeled using volume elements with eight isoparametric elements with linear interpolation functions over the gusset plate thickness. The RHS-member in the joint region was modeled using shell elements with 20 elements for each section wall. The welds between the gusset plate and member are not modeled in detail, implying meaning the execution of butt welds. The sealing plates (see Fig. 1, 3) were omitted. The rest of the member outside the joint was modeled using beam elements with a rigid kinematic coupling to the shell elements.

The boundary conditions in axis I were based on the studied cases, pinned or fully clamped out of plane.

Within the calculations member lengths of L_0 = 4,8 and 12 m were considered with a member section RHS 200/200/10 mm without fillets (leading to A_0 = 7600 mm², r_{z0} = 78 mm).

In all calculations, a linear elastic-ideal plastic material behaviour without strain-hardening was chosen, with a yield stress F_y = 235 N/mm². This leads to an ultimate section capacity of $N_{0,pl}$ = $A_0 \cdot F_y$ = 1.786 kN. An elastic modulus of E = 210.000 N/mm² and a Poisson's ratio of υ = 0,3 were selected.

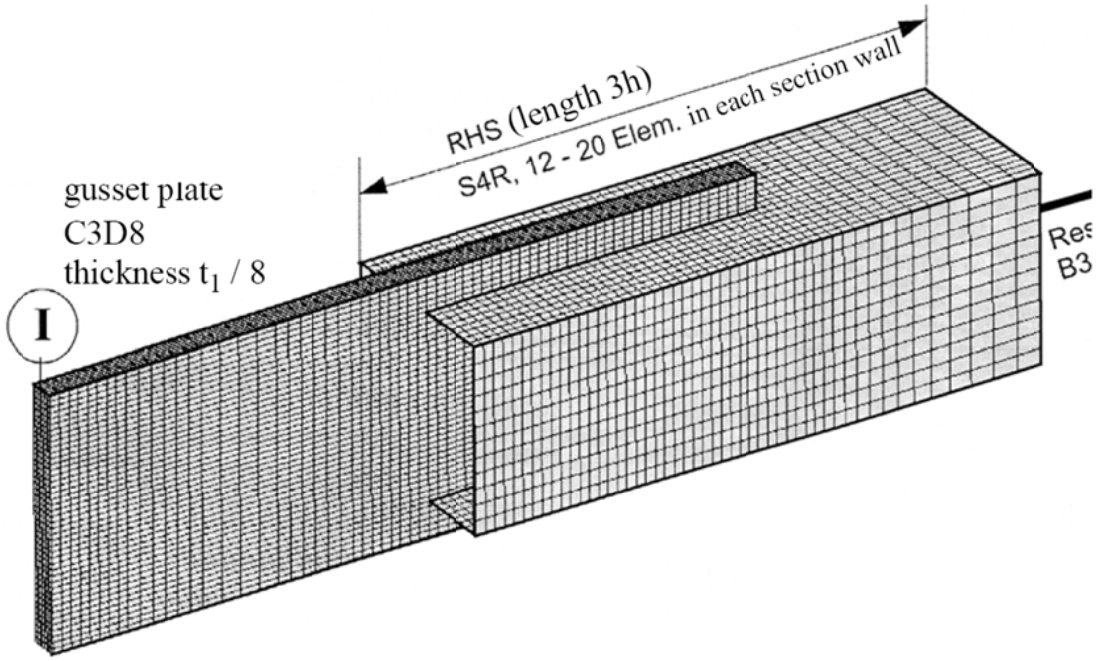

Figure 8: FEM numerical model for the calculation of the load bearing capacity

4.2 Linear buckling Analyses

For each studied member, a linear buckling analyses (LBA) was performed prior to the non-linear calculations, due to the fact that the calculated buckling modes also formed the basis for the selected geometric imperfections (1st and 2nd mode studied).

Fig. 9 shows the first and second buckling modes for a member with L_0 = 8000 mm and pinned as well as fully clamped ends of the gusset plate.

The comparison of the ideal buckling loads $N_{cr,i}$ based on the LBA analyses with the ones calculated using beam-theory (Eq. (3) with effective length factors of Fig. 5) shows a overestimation by the latter. This is understandable as a consequence of the local load introduction from the gusset plate to the member, making the first portion of the RHS member bending stiffness partially ineffective, leading to an overestimation of $N_{cr,i}$.

Based on a comprehensive study by the authors, it is suggested - for practical applications - to increase the – computational - free length of the gusset plate L_1 (used to determine $N_{cr,i}$ on the basis of beam-theoretical methods such as the one represented by Fig. 5) by a distance ΔL_1 = b/5 = h/5. This leads to an increased length L_1^* = L_1 + h/5 if the effective length factors of Fig. 5 are used (new parameter L_1^*/L_0).

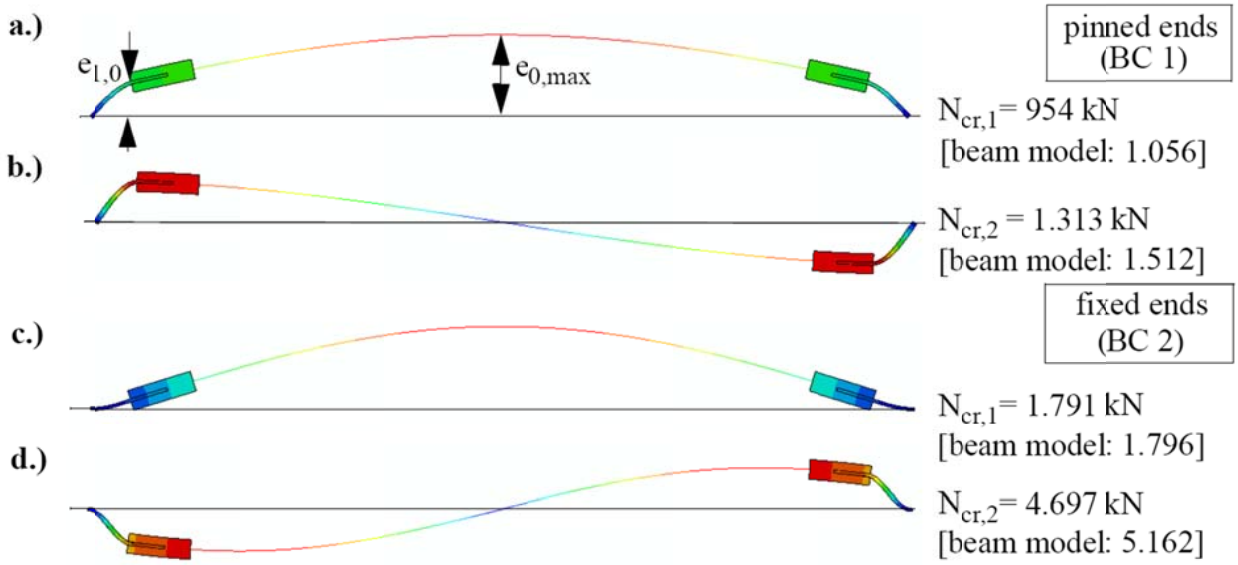

Figure 9: Different buckling modes (FEM-Model) for a member with L_0 = 8 m (Profile RHS 200/200/10; gusset plate 260/28; L_1 = 400 mm)

4.3 Realistic compression load bearing behaviour

For the calculation of realistic compression strength values of the member with slotted gusset plates, a series of GMNIA-analyses (geometric and material nonlinear analyses with imperfections) was carried out.

In a first step, LBA-analyses were performed. The calculated eigenmodes (1st and 2nd) were selected for the imperfection shape along the member. These shapes were then scaled, with the maximum value of the imperfection chosen with $e_{0,max}$ = L_0/750, based on the code of execution EN 1090-2 (2008) now used in Europe, which gives measurements that are relevant for both eigenmode shapes.

In addition, the effect of an inclination angle of φ_{max} = 1/100 of the gusset plate was considered as well, leading to the four different shapes of imperfection, summarized in Fig. 10.

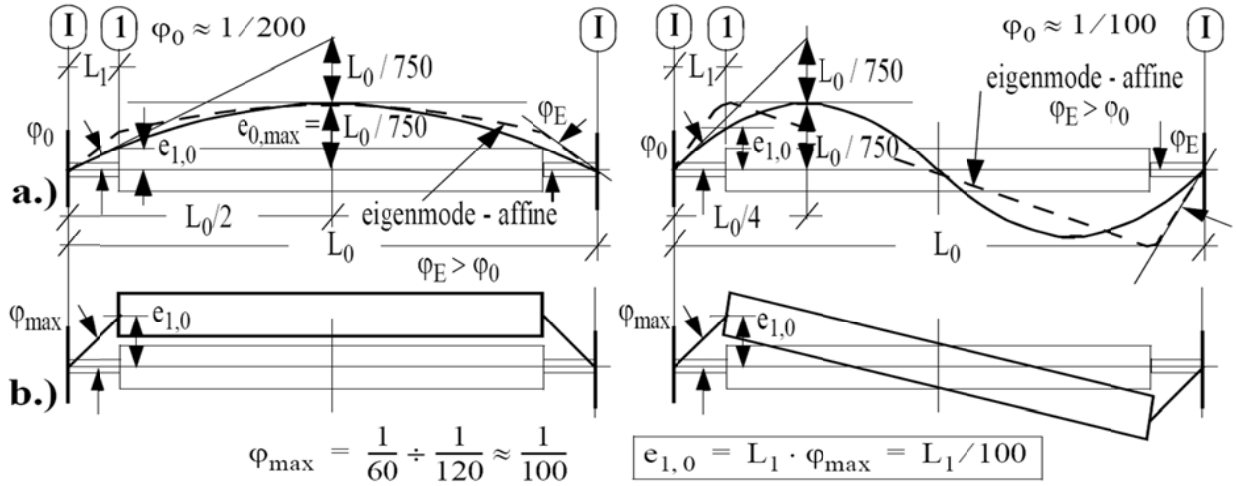

Figure 10: Realistic assumptions of geometric imperfections, based on executive codes; a.) EN 1090-2 (2008) and b.) EN ISO 13920 (1996)

4.4 Impact of additional residual stresses due to welding

The impact of additional residual stresses was also studied in this paper, due to relevance of the welding connection between gusset plate and the member. For the distribution of the residual stresses, a rather conservative approach was selected, leading to residual stresses reaching the yield stress along the elements near the weld (simulation of the residual stresses by a temperature load case ΔT). Fig. 11 shows the results for a member with L_0 = 4000 mm. The stress distributions in section A, B, C of the gusset plate are plotted in Fig. 11c (residual stresses σ_E and ultimate stresses σ_0 and σ_u at top and bottom surface of the gusset plate). In Fig. 11b, the load-deformation behavior – with and without residual stresses – is presented. Although a very conservative approach for the residual stress pattern was made, only a moderate decrease of the ultimate capacity of approximately 10 % (609 kN instead of 668 kN in Fig. 11) was observed. This effect will be considered in the design approach in section 5 in form of an increased geometric imperfection (factor f_{equ}).

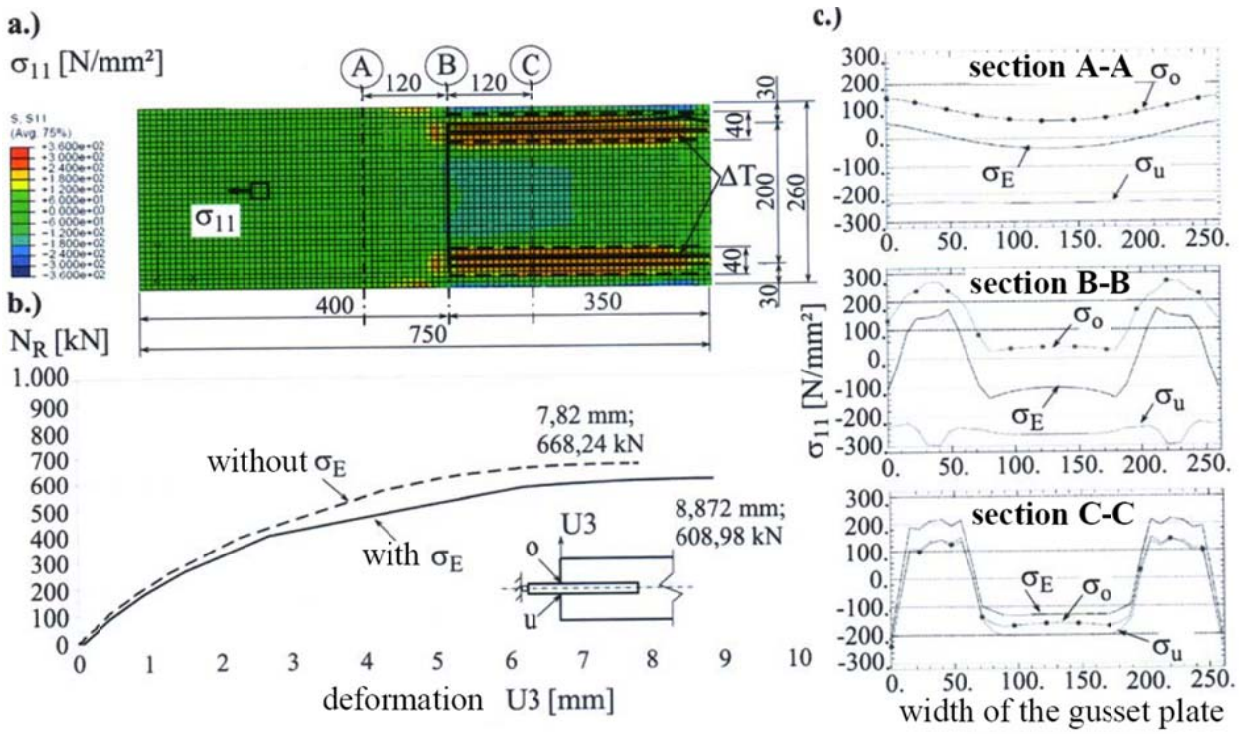

Figure 11: Load bearing capacities and considered residual stresses σ_E for a member with L_0 = 4000 mm and pinned ends (geometric imperfections based on the 1st buckling mode shape)

5. Suggestion of a design model for practical application

Based on the results of the GMNA-calculations for the studied members with slotted gusset plates, the authors developed a simple design model for practical design. The background of this model, summed up in section 5.2, will be shown in the following.

5.1 Design model for compressive strength considering the limited section capacity of the gusset plate

As shown for the example in Fig. 7, the compressive strength of the member is often limited due to the limited section capacity of the gusset plate in its cross-section 1.

The main idea of the design model, based on 2nd order theory, is summed up in Fig. 12 for a member with pinned ends. The plot shows the deformation U_3 (out-of-plane) in the gusset plate at the end of the member (section 1) with increasing axial load N. The circles represent the "realistic" behaviour, determined by GMNIA-calculations.

Starting from the geometric imperfection $e_{1,0}$ at the member end in section 1, the deformation (U_3 in Fig. 12) increases following the elastic 2nd order amplification factor given by Eq. (4), i.e. the factor f_{II} that accounts for the correct ideal buckling load P_{cr}, nearly up to the ultimate load ($U_3 = e_{1,0} \cdot f_{II}$).

In addition, the section capacity of the gusset plate is also represented in Fig. 12 by the descending lines, leading to reduced axial load carrying capacites N if the deformation U_3 increases (due to additional moment $M^{II} = N \cdot U_3$). As border lines the (too high) fully (i.e. non-linear) plastic and the (too low) linear-elastic cross-sectional capacity curves for the rectangular

gusset plate section are shown. If a reduced plastic capacity curve – with a linear interaction between axial force and bending moment - is used for the gusset plate, the intersection point with the deformation curve ($U_3 = e_{1,0} \cdot f_{II}$) gives the result of the design model ($N/N_{pl,RHS} = 0{,}28$ in Fig. 12).

This compressive strength is in good agreement with the real ultimate load of approximately $N/N_{pl,RHS} = 0{,}29$, albeit the latter features higher deformations $U_3 = 20$ mm.

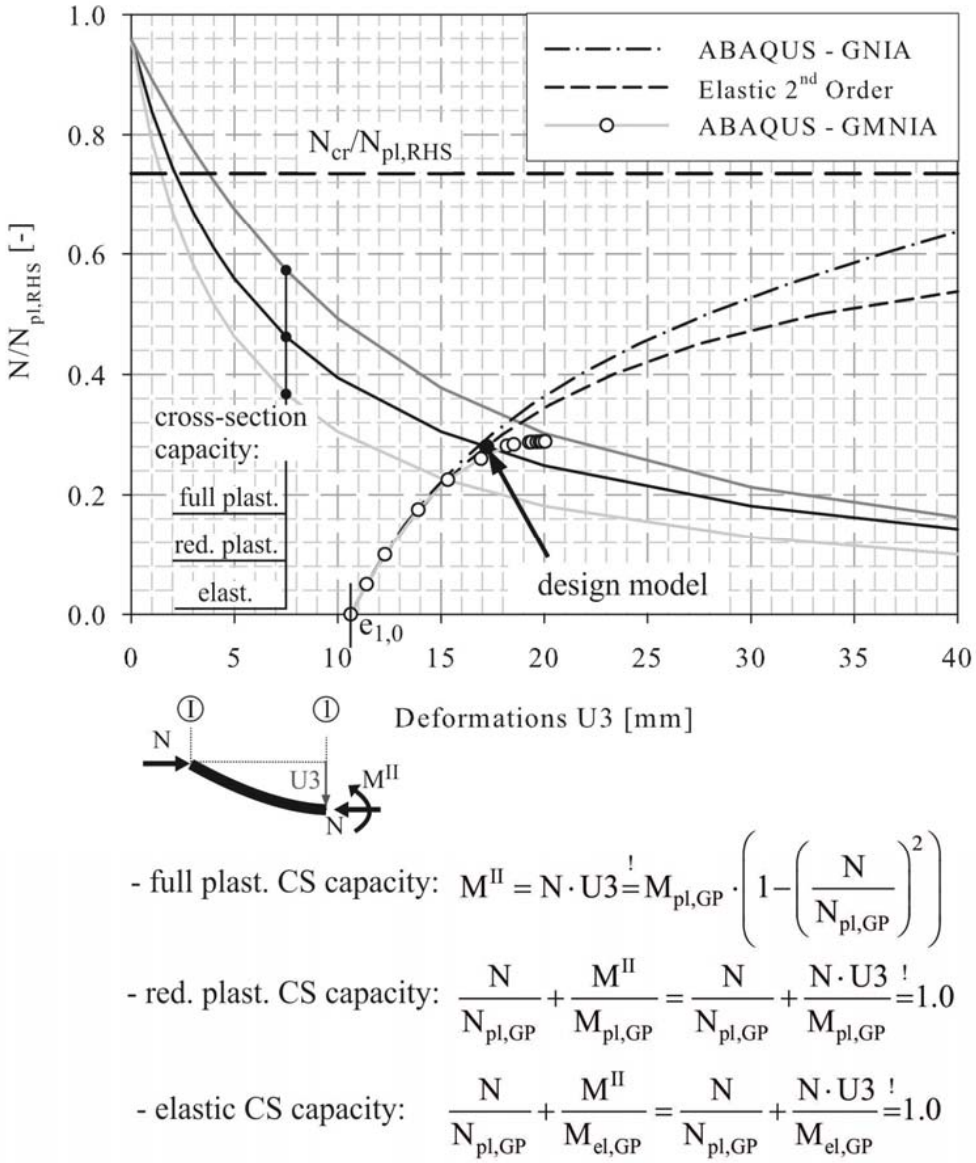

Figure 12: Deformation and cross-sectional resistance at the relevant gusset plate section for pinned ends

This simple design model works for all types of geometrical imperfections (as described in Fig. 10) and for both buckling modes. It is worth mentioning that - for the deformation U_3 based on

the simple elastic 2nd order amplification factor, the relevant ideal buckling load $N_{cr,i}$ must always be considered.
Table 1 summarized some additional examples. The results of the simple engineering design model ($N_{Eng.model}$) are compared with the FEM-calculations (N_{GMNIA}).

It can be seen that - for the eigenmode-affine imperfections, with equal amplitudes, see Fig. 10a- nearly in all cases the 2nd modes lead to the lower ultimate compressive strength.

In the case of a member with clamped ends at the gusset plate (BC2 in Fig. 3), the design model is more complex due to the fact that the overall moment M_{ges} caused by the deformation w_1 at the member end must be splitted in two individual parts for the two relevant sections I and 1, see Fig. 13.

Table 1: Load bearing capacities N_R [kN] for the variation of geometric imperfection shapes only (based on Fig. 10); RHS 100/200/10, t_1 = 28, L_1 = 400 mm

end support	length L_0 [m]	$N_{cr,1}$ $N_{cr,2}$	eigenmode-affine; $e_{0,max} = L_0/750$			Gusset plate inclination		
			$e_{1,0}$ [mm]	N_{GMNIA} [kN]	$N_{Eng.model}$ [kN]	$e_{1,0}$ [mm]	N_{GMNIA} [kN]	$N_{Eng.model}$ [kN]
BC 1 pinned	4,0	1.184	4,51	**670**	680 (+1,5 %)	4,0	**697**	707 (+1,4 %)
		1527	5,33	707	708 (+0,1 %)	4,0	772	786 (+1,8 %)
	8,0	954	4,45	611	615 (+0,7 %)	4,0	**646**	633 (-2,0 %)
		1.313	10,6	**514**	497 (-3,3 %)	4,0	726	740 (+1,9 %)
	12,0	595	2,78	497	497 (0 %)	4,0	**521**	467 (-10,4 %) [1]
		1.213	14,6	**430**	412 (-4,2 %)	4,0	700	716 (+2,3 %)
BC 2 fully clamped	4,0	4.642	3,27	1.386	1.361 (-1,8 %)	4,0	1.373	1.300 (-5,3 %)
		5.199	5,32	**1.241**	1.217 (-2,0 %)	4,0	**1.340**	1.313 (-2,0 %)
	8,0	1.791	1,13	1.213	1.357 (+12 %)	4,0	**1.312**	1.064 (-19 %) [1]
		4.697	8,65	**1.086**	1.012 (-6,8 %)	4,0	1.351	1.302 (-3,6 %)

1. not relevant, because buckling of the member determined (section m)

The proposed design model for this cases focuses now on section I, because at this location a design verification of the welded connection is needed as well. The moment in section I can conservatively be estimated to amount to about 70 % of M_{ges}, due to the fact that the simple engineering model underestimates the deformation w_1 by using f_{II}. In partial compensation of this error, it can be shown that at section I the full plastic section capacity can be utilized.

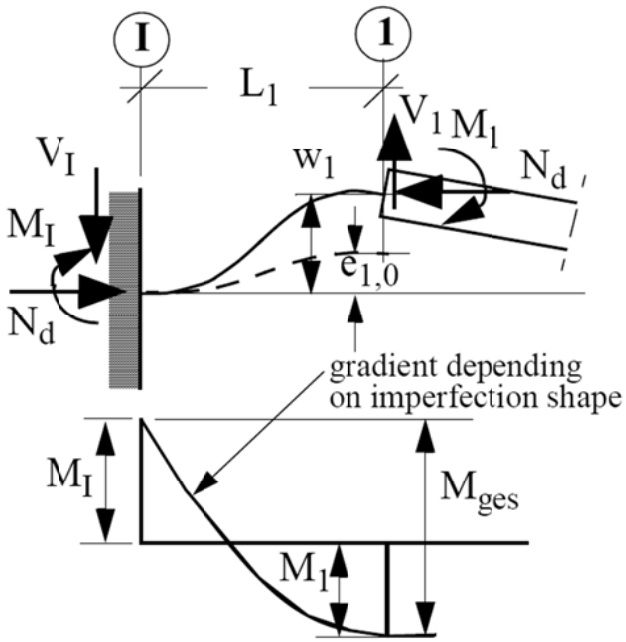

$$M_{ges} = N_d \cdot w_1 = N_d \cdot e_{1,0} \cdot f_{II}$$

$$f_{II} = 1/(1 - N_d/N_{cr})$$

$$M_{ges} = M_I + M_1$$

$$V_1 = M_{ges}/L_1$$

Figure 13: Engineering model for the calculation of the load bearing capacity N_d for fixed ends

5.2 Summary of the suggested design model for the compression strength of members with slotted gusset plates

Summing up the results of section 4 and 5.1, a design model for the calculation of the compression strength of members with slotted gusset plates is now available.

This design model can be adapted to different national codes, which may have different rules (particularly, buckling curves and tolerance requirements) for column buckling verifications against axial compression forces N_d. For a better understanding of the proposal, in the following representation of the design model all safety factors are omitted.

The verification of the member contains two individual checks - both must be fulfilled. Alternatively, for each verification a maximum compression strength can be determined (utilization factor equal to 1,0) – the minimum of both gives the resulting compression capacity of the member.

- Verification 1: buckling check of the member

– Conventional buckling check, based on an increased effective buckling length for the 1st buckling mode ($L = \beta_1 \cdot L_0$, see Fig. 5)

– For the calculation of the effective length factor β_1 using e.g. the graphs in Fig. 5, an increased length $L_1^* = L_1 + h/5$ should be used

– Note: Verification 1 checks the member in the region near midspan against second-order internal forces (compression + bending) exceeding the section capacity

- Verification 2: additional verification of the section capacity of the gusset plate

a) geometric imperfection at the gusset plate (section 1)
$e_{1,0} = L_1/100 \geq 2$ mm

Note: Based on execution codes EN 1090-2 (2008) and EN ISO 13920 (1996). Different imperfection amplitudes may be considered on the basis of other national or industry-specific tolerance requirements.

b) geometric equivalent imperfections at the gusset plate (section 1)
$e_{1,equ} = f_{equ} \cdot e_{1,0} = 2.0 \cdot e_{10} = 2.0 \cdot L_1/100 \geq 4$ mm
Note: The factor f_{equ} is a very conservative assumption, based on the study of the effects of residual stresses due to welding of the connection between gusset plate and member.

c) verification
- pinned ends (BC1): (only reduced plastic section capacity available)

$$N_d \cdot e_{1,equ} \cdot \frac{1}{1-N_d/N_{cr,1}} \leq M_{1,pl,Rd} \cdot \left(1 - N_d/N_{1,pl,Rd}\right) \quad (5)$$

- fully clamped ends (BC2):

$$0{,}7 \cdot N_d \cdot e_{1,equ} \cdot \frac{1}{1-N_d/N_{cr,1}} \leq M_{1,pl,Rd} \cdot \left(1 - \left(N_d/N_{1,pl,Rd}\right)^2\right) \quad (6)$$

- End moment M_I (basis for weld connection design)

$$M_{Id} = 0{,}7 \cdot N_d \cdot e_{1,equ} \cdot \frac{1}{1-N_d/N_{cr,1}} \quad (7)$$

Note 1: - the ideal buckling load $N_{cr,1}$ for the 1st mode must always be used
Note 2: - the plastic section capacity $M_{1,pl,Rd}$ and $N_{1,pl,Rd}$ of the gusset plate are defined (with F_{yd} … design value of the yield stress), respectively:

$$M_{1,pl,Rd} = \frac{h_1 \cdot t_1^2}{4} \cdot F_{yd};\ N_{1,pl,Rd} = h_1 \cdot t_1 \cdot F_{yd}$$

References

Zhao, R., Huang, R., Khoo, H.A., Cheng, J.J.R. (2009). "Parametric finite element study on slotted rectangular and square HSS tension connections". *Journal of constructional steel research*, 65 611-621.

Unterweger, H. (2010). "Load bearing capacity of bracing members with almost centric joints". *Proceedings of Int. conference stability and ductility of steel structures – SDSS*, Rio de Janeiro, 603-610.

Unterweger, H., Taras, A. (2011). "Hohlprofile mit beidseits zentrisch eingeschlitzten Knotenblechen – Drucktragverhalten und Bemessungsvorschlag." *Stahlbau*, Band 680, Heft 11, 839-851.

Eurocode EN 1993-1-1 (2012). "Eurocode 3; Design of Steel Structures – Part 1-1: General rules and rules for buildings."

Eurocode EN 1090-2 (2008). "Execution of steel structures and aluminium structures – Part 2: Technical requirements for steel structures."

EN ISO 13920 (1996). "Welding – General tolerances for welded constructions – Dimensions for lengths and angles, shape and position."

Petersen, Ch. (1982). "Statik und Stabilität der Baukonstruktionen". *Vieweg & Sohn*, 2. Auflage.

Pflüger, A. (1964). "Stabilitätsprobleme der Elastostatik", *Springer Verlag*, 2. Auflage.

Dimitrov, N. (1953). "Ermittlung konstanter Ersatz-Trägheitsmomente für Druckstäbe mit veränderlichen Querschnitten". *Der Bauingenieur*, 28, H6, 208-211.